BIOCHEMISTRY
including biophysical chemistry & molecular biology

ARTICLE

pubs.acs.org/biochemistry

Solution NMR Insights into Docking Interactions Involving Inactive ERK2

Andrea Piserchio,[†] Mangalika Warthaka,[‡] Ashwini K. Devkota,[§] Tamer S. Kaoud,[‡,∥] Sunbae Lee,[‡] Olga Abramczyk,[‡] Pengyu Ren,[§,⊥] Kevin N. Dalby,[*,‡,§,∥,⊥,#] and Ranajeet Ghose[*,†,&]

[†]Department of Chemistry, The City College of New York, New York, New York 10031, United States

[‡]Division of Medicinal Chemistry and Graduate Programs in [§]Cellular and Molecular Biology, [∥]Pharmacy, [⊥]Biomedical Engineering, and [#]Biochemistry, University of Texas, Austin, Texas 78712, United States

[&]The Graduate Center of CUNY, New York, New York 10016, United States

Supporting Information

ABSTRACT: The mitogen-activated protein (MAP) kinase ERK2 contains recruitment sites that engage canonical and noncanonical motifs found in a variety of upstream kinases, regulating phosphatases and downstream targets. Interactions involving two of these sites, the D-recruitment site (DRS) and the F-recruitment site (FRS), have been shown to play a key role in signal transduction by ERK/MAP kinases. The dynamic nature of these recruitment events makes NMR uniquely suited to provide significant insight into these interactions. While NMR studies of kinases in general have been greatly hindered by their large size and complex dynamic behavior leading to the suboptimal performance of standard methodologies, we have overcome these difficulties for inactive full-length ERK2 and obtained an acceptable level of backbone resonance assignments. This allowed a detailed investigation of the structural perturbations that accompany interactions involving both canonical and noncanonical recruitment events. No crystallographic information exists for the latter. We found that the chemical shift perturbations in inactive ERK2, indicative of structural changes in the presence of canonical and noncanonical motifs, are not restricted to the recruitment sites but also involve the linker that connects the N- and C-lobes and, in most cases, a gatekeeper residue that is thought to exert allosteric control over catalytic activity. We also found that, even though the canonical motifs interact with the DRS utilizing both charge−charge and hydrophobic interactions, the noncanonical interactions primarily involve the latter. These results demonstrate the feasibility of solution NMR techniques for a comprehensive analysis of docking interactions in a full-length ERK/MAP kinase.

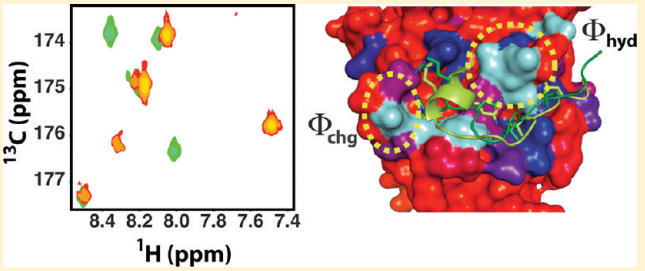

Extracellular signal-regulated kinases (ERK) constitute a subfamily of mitogen-activated protein (MAP) kinases that undergo up-regulation upon activation of cell surface receptors by extracellular events such as binding of cytokines or growth factors.[1−3] ERKs play a central role in growth-factor-related apoptosis in colorectal cancer,[4] and the ERK signaling pathway is a key target for anticancer therapeutics.[5,6] Activation of ERKs (ERK1 and ERK2) occurs downstream of the Ras/Raf pathway upon dual phosphorylation of a conserved T−X−Y motif (^{183}T−X−Y^{185} in ERK2) in the activation loop by MAPKKs (MAP/ERK kinase kinase). Activated ERKs phosphorylate a host of downstream targets both in the cytosol[7,8] and in the nucleus.[9] Down-regulation of enzymatic activity occurs by single or dual dephosphorylation by serine/threonine, tyrosine, or dual-specificity phosphatases.[3] ERKs (see Figure 1) possess a catalytic domain containing the archetypal motifs present in protein kinases[10,11] but do not possess any additional regulatory domains unlike, for example, the Src-family kinases.[12] A feature of MAPKs (including ERKs) is the presence of the so-called "MAP kinase insert" between the αG and αH helices and of an α-helical C-terminal extension (see Figure 1). The MAP kinase insert has been deemed to be important in protein−protein interactions involving a host of regulators[13,14] and substrates.[15]

MAP kinases, including ERK1/2, utilize specific docking or recruitment sites distinct from the active site to recognize substrate or regulatory motifs.[16,17] These regulatory interactions occur with up-regulating MAPKKs, adaptor proteins, and down-regulating phosphatases.[18] Among the best-characterized MAP kinase-docking motifs is one variously known as a D-site, D-motif, kinase interaction motif (KIM), or DEJL motif, which contains a conserved $(R/K)_{2-3}-X_{2-6}-\Phi_A-X-\Phi_B$ sequence (Φ_A and Φ_B are hydrophobic residues). Crystal structures of MAP kinases complexed with D-site peptides have revealed insights into the structural basis of these interactions.[19] These studies have shown that basic residues of the D-site bind to a negatively charged surface (Φ_{chg}, containing two common-docking

Received: January 13, 2011
Revised: March 29, 2011
Published: March 30, 2011

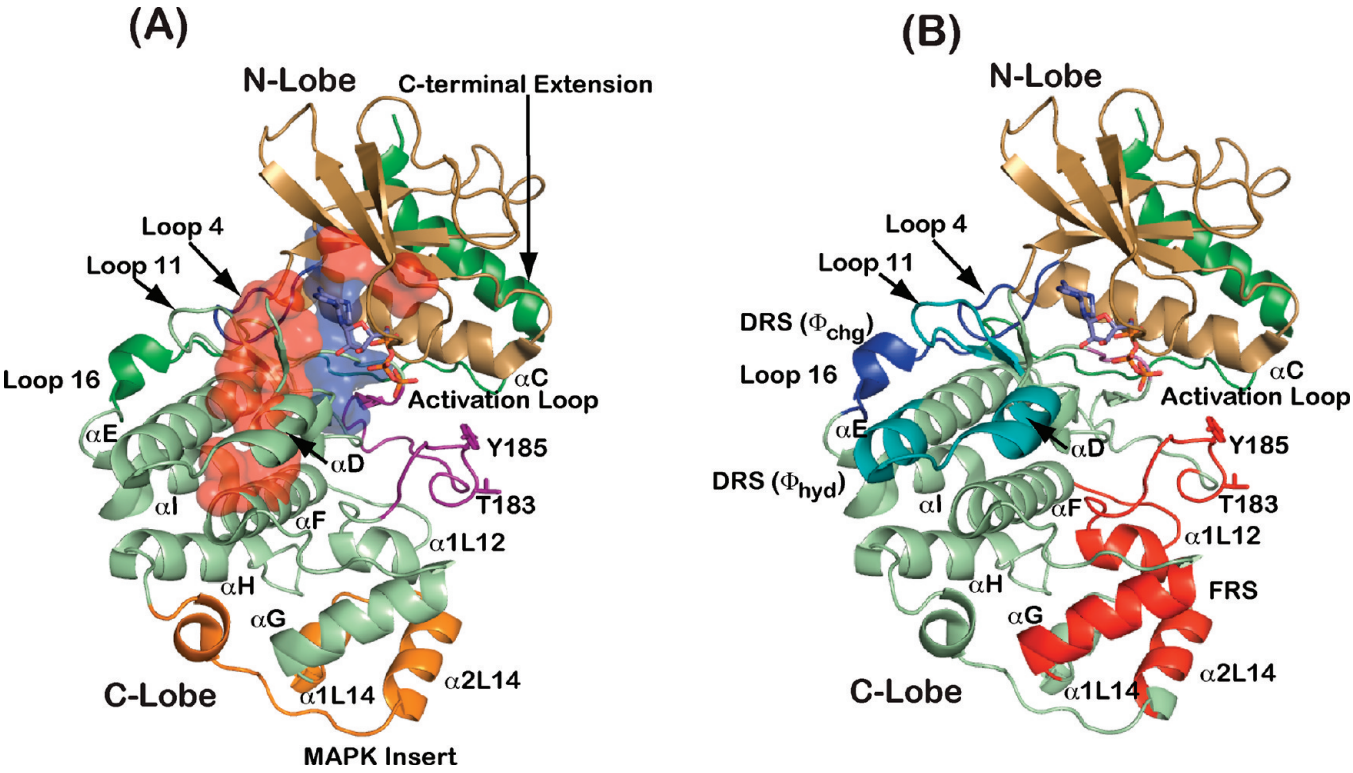

Figure 1. Ribbon representation of the structure of ERK2. (A) The N- and C-lobes are colored gold and light green, respectively. The MAP kinase insert is colored gold, and the C-terminal helix is colored green. The activation loop bearing the catalytic T183 and Y185 (indicated in stick representation) is colored magenta. The so-called R- and C-spines are shown as surfaces and colored red and blue, respectively. These two spines rest on the αF helix, which, along with other key helices, is labeled. (B) The D-recruitment site (DRS) and the F-recruitment site (FRS) are shown. The FRS is colored red; the Φ_{chg} subsite of the DRS is colored blue, and the Φ_{hyd} subsite is colored cyan. A bound ATP molecule is shown in stick representation.

Asp residues[20]), and the $\Phi_A-X-\Phi_B$ sequence binds to a nearby hydrophobic docking (Φ_{hyd}) pocket on the surface of the kinase. These two sites, Φ_{chg} and Φ_{hyd}, constitute the D-recruitment site (DRS) on ERK2. It has been shown that binding at the DRS can induce long-range conformational changes in the kinase.[17,21−23] Structures of ERK2 bound to D-site peptides from the phosphatases MKP3[23] and HePTP[24] showed similar conformational transitions of the activation loop, which adopted a configuration similar to the active state. Recent results suggest a role for D-site interactions in the allosteric regulation of kinase activity in ERKs.[25] In addition, a second docking motif deemed important for target recognition has been identified.[21] The "DEF" motif (docking site for ERK FXFP) or F-site contains a F-X-F-P sequence that is conserved in multiple ERK targets including Elk-1, c-Fos, SAP1, and the kinase suppressor of Ras (KSR). A library-scan analysis suggests that either F in the FXFP motif may be substituted for Y or W.[26] Unlike the DRS, no clear crystallographic information exists for the nature of interactions that define the F-recruitment site (FRS). However, key residues that define this site have been identified using hydrogen exchange mass spectrometry (HXMS) coupled with mutational analysis.[21] It was shown that Y231, L232, and L235 on one side of a hydrophobic groove on ERK2 together with M197, L198, and Y261 were crucial in defining the FRS and interacting with F-site sequences. Mutation of the residues Y231, L232, L235, and Y261 to Ala in active ERK2 leads to significant reduction in binding.[21] These data allowed a model of an F-site peptide from Elk-1 bound at the FRS to be obtained.[21] It was also suggested that this site is only partially formed in inactive ERK2. However, at least partial use of this site, both in the active and in the inactive enzyme, has been noted for the transcription factor Ets-1, an ERK2 substrate which lacks a canonical F-site sequence.[27] In addition, the antiapoptotic adaptor protein PEA-15, which also lacks a canonical F-site sequence, has been suggested to bind at a site proximal to the FRS in both active and inactive ERK2.[14,28] In both cases the DRS is also extensively involved in promoting these noncanonical interactions.[28,29]

Given the central importance of these docking interactions, their structural and dynamic characterization is crucial for understanding their role in the regulation of MAP kinase signal transduction pathways (e.g., in ERK2). This is especially true for the noncanonical ligands described above, for which extensive biochemical information,[14,15,21,27,28] but no structural data, is available. Several of these noncanonical interactions involve intrinsically disordered segments that likely retain a substantial portion of their flexibility after complex formation.[27,28] This is a possible reason why the complexes have evaded crystallization. Given these issues, solution NMR techniques seem ideally suited to study docking interactions involving ERK/MAP kinases. NMR studies are expected to enhance and expand crystallographic information available for canonical D-site interactions in the ERK/MAP kinase family, providing information about variability in these associations involving different D-site ligands. For interactions that involve canonical F-site sequences and noncanonical ligands, these studies are expected to confirm mutational analyses and allow their interpretation in structural terms. The large size of the ERK/MAP kinases (>40 kDa), their instability under the high concentrations required for NMR experiments, and their complex dynamics lead to a failure of conventional techniques for resonance

dx.doi.org/10.1021/bi2000559 |*Biochemistry* 2011, 50, 3660–3672

assignment. This is a common problem in the NMR studies of protein kinases, and therefore only a handful of NMR analyses of these key signaling enzymes have appeared in the literature. These include protein kinase A,[30,31] the catalytic domain of c-Abl,[32] the ERK2 homologue p38α,[33,34] and the catalytic domain of the Eph receptor tyrosine kinase.[35]

Given that for ERK2 extensive structural, biochemical, and functional information on docking interactions is available, we undertook the task of obtaining resonance assignments to investigate the structural and dynamic effects of these interactions. Here, as a first step toward this goal, we present an analysis of canonical and noncanonical docking interactions involving full-length inactive ERK2 using solution NMR techniques. Our studies demonstrate the feasibility of using solution NMR methodology to study protein−protein interactions involving a full-length ERK/MAP kinase and represent the very first comprehensive NMR analysis of protein−protein interactions for the ERK/MAP kinase family. Our results provide unique insight into the variability of these interactions and also into the network of connectivity that propagates from the recruitment sites into remote regions of the protein. They also confirm the results of the mutational analyses and demonstrate that interactions involving sequences that do not carry canonical D- or F-sites can also engage the DRS and FRS.

MATERIALS AND METHODS

Protein Expression and Purification. BL21 (DE3)-T1 competent *E. coli* cells were transformed with a pET28 vector coding for an N-terminal His_6 tag, a thrombin cleavage site, and the sequence of full-length rat ERK2 (Kaoud, T. S. et al., manuscript in preparation). Starting from a fresh transformation, cells were grown overnight in 20 mL of M9 media in a shaking incubator (37 °C, 250 rpm). The following day, the cells were diluted with fresh media to prepare 10 mL of an M9 culture containing 10% D_2O, with a starting OD_{600} of 0.2. When the OD_{600} reached 0.6, the cells were diluted by a factor of 2 using a stock of M9 media in 100% D_2O (10 mL total volume). This operation was repeated several times until the cells were adapted for growth in 98% D_2O. For all the adaptation steps, 8 g/L glucose and 1 g/L ammonium chloride were used. The adapted cells were then used to inoculate a new M9 culture prepared in 100% D_2O containing 5 g/L ^{13}C, ^{2}H glucose, and 1 g/L $^{15}NH_4Cl$ and were incubated overnight. The cells were used the following morning to inoculate 0.5 L M9 medium prepared in 100% D_2O containing 3 g/L $^{2}H,^{13}C$ glucose and 1 g/L $^{15}NH_4Cl$. At an OD_{600} of 0.6, the cells were transferred on ice for 0.5 h, induced with 400 μM IPTG to overexpress uniformly ^{2}H, ^{15}N, and ^{13}C-labeled ERK2, and transferred into a shaking incubator set to 17 °C for 24 h. The cells were then spun down at 7000*g* and stored at −80 °C for future manipulations. All media were supplemented with 50 mg/L of kanamycin.

Samples containing amino acids selectively ^{13}CO-labeled in a uniformly $^{2}H,^{15}N$-labeled background were produced following the protocol developed by Takeuchi and co-workers.[36] Briefly, the same recipe described above was applied with the following modifications: $^{2}H,^{12}C$ glucose was used for both the final overnight and for the final large-scale growth. For the latter step, 1.5 g/L of $^{2}H,^{12}C$ glucose was used, together with 1.5 g/L of $^{2}H,^{15}N$-labeled Celtone base powder (Cambridge Isotope Laboratories Inc.) When the OD_{600} reached 0.6, specific $^{1}H,^{14}N,^{12}C,^{13}CO$-labeled amino acids (as required) were added individually to the growth medium. The following amounts were used (depending on which specific amino acid was being selectively ^{13}CO-labeled): Ala, 212 mg/L; Gly, 178 mg/L; Ile, 87 mg/L; Leu, 233 mg/L; Val, 125 mg/L. After 0.5 h of incubation in a shaker at 37 °C, the cells were put on ice for 0.5 h, induced with 400 μM IPTG, and transferred into the shaking incubator at 17 °C. After ∼16 h of induction, selectively labeled amino acids were added to the growth in the amounts mentioned above. The cells were spun down and stored after growth for 24 h. In the case of Leu and Val selective labeling, 250 mL of media was used for the final growth.

For purification, the cells were thawed on ice and resuspended in 20 mL of lysis buffer (50 mM Tris, pH 7.5, 750 mM NaCl, 0.5% Triton, 0.1% β-mercaptoethanol, 1 Roche protease inhibitor cocktail tablet), passed three times through a French pressure cell, and centrifuged at 75000*g*. The supernatant was then incubated with 5 mL of Co^{2+} resin (TALON, Clontech) under gentle agitation at 4 °C for 0.5 h, then loaded onto a column, washed multiple times, first with lysis buffer, then with wash buffer (50 mM Tris, 150 mM NaCl at pH 7.5), then again with wash buffer containing 3 mM imidazole, and finally eluted with wash buffer containing 200 mM imidazole. The protein was dialyzed against 20 mM Tris, 150 mM NaCl, 2.5 mM $CaCl_2$, 0.1% β-mercaptoethanol, pH 8.3, and the His_6 tag was cleaved using 2 units/mg of human α-thrombin (Enzyme Research Laboratories). The completeness of the cleavage was monitored using 20% SDS gels. Adding 200 mM AEBSF and 5 mM DTT stopped the cleavage reaction. The protein was concentrated using AMICON (Milipore) concentrators and loaded onto a gel filtration column (Sephacryl S-100 HR) pre-equilibrated with the NMR buffer (50 mM phosphate, 150 mM NaCl, 2 mM DTT, 500 μM EDTA, pH 6.8). The concentration of ERK2 in the NMR samples was kept around 200 μM for greater stability.

NMR Experiments. All NMR spectra were recorded at 25 °C. Typically ∼200 μM inactive ERK2 in NMR buffer containing 10% D_2O was loaded into a 5 mm Shigemi tube susceptibility-matched to water. Spectra were collected at multiple fields (600, 700, 800, and 900 MHz) on Bruker Avance spectrometers or on a Varian Inova operating at 600 MHz. All spectrometers were equipped with cryogenic probes capable of applying pulsed field gradients along the *z*-axis. Triple resonance experiments were collected both in the presence and absence of 10 mM $MgCl_2$ and 4 mM ADP. TROSY versions[37] of the following triple resonance experiments were collected: HNCO (800 MHz, with and without Mg^{2+}/ADP), HNCACB (800 MHz, with Mg^{2+}/ADP; 900 MHz, without Mg^{2+}/ADP), HNCA (700 MHz, without Mg^{2+}/ADP; 800 MHz, with Mg^{2+}/ADP), HN(CO)CA (600 MHz with and without Mg^{2+}/ADP), and HN(CA)CO (800 MHz, only for the Mg^{2+}/ADP state). 3D ^{15}N-edited NOESY-TROSY experiments with mixing times of 120 ms (600 MHz, no Mg^{2+}/ADP), 180 ms, and 400 ms (800 MHz, with Mg^{2+}/ADP) were also collected. ^{15}N-, ^{1}H TROSY-, and TROSY-based HNCO experiments were also collected for each sample grown in the presence of specific ^{13}CO-labeled amino acids (Leu, 800 MHz with Mg^{2+}/ADP; 700 MHz, without Mg^{2+}/ADP; Val, 800 MHz, without Mg^{2+}/ADP; Ile, 900 MHz, without Mg^{2+}/ADP; Ala 800 MHz. with Mg^{2+}/ADP; Gly 600 MHz, with Mg^{2+}/ADP). Substoichiometric amounts (1:0.25 or 1:0.5) of a spin-labeled ATP (sl-ATP) analogue (that contained a mixture of species nitroxide-labeled at the ribose 3′: 70%−80%, or the ribose 2′: 20−30%, a kind gift from Dr. Pia D. Vogel) was added to a 200 μM ERK2 NMR sample containing 5 mM $MgCl_2$ (in NMR buffer prepared without DTT). ^{15}N, ^{1}H TROSY, and

TROSY-HNCO experiments were recorded before and after addition of the sl-ATP, and the effects of the spin-label were evaluated by analyzing the ratios of peak intensities. Drawbacks of using this simple approach for quantitative analyses of paramagnetic relaxation enhancement (PRE) effects have been noted;[38] however, it is sufficient for our case since the PRE data were only used qualitatively. To aid the resonance assignment procedure, chemical shifts were predicted from the known crystal structures (PDB IDs: 1ERK and 3ERK) using the program Sparta[39] and manually corrected for ^{2}H isotope effects on ^{13}C chemical shifts.[40] Details of the procedures used for resonance assignment will be described elsewhere.[41]

Docking Interactions with Inactive ERK2. Chemical shift perturbations in inactive ERK2 in the presence of the following ERK2 ligands were analyzed:

(a) FQRKTLQRRNLKGLNLNL-$(\Delta)_3$-TGPLSPGPF, an 18-residue peptide bearing a D-site sequence from the yeast MAPKK Ste-7 separated from a 9-residue substrate segment by chain consisting of three 6-aminohexanoic acid (Δ) spacers.

(b) A 17-residue peptide derived from the N-terminus of the transcription factor Elk-1 bearing a D-site sequence: QKGRKPRDLELPLSPSL.

(c) A construct consisting of the N-terminal 138 residues from the transcription factor Ets-1 (Ets-1 Δ138, referred to as *Ets* for simplicity).

(d) The full-length 15 kDa adaptor protein PEA-15 (phosphoprotein enriched in astrocytes).

The synthesis of peptide (a) will be described elsewhere (Lee et al., manuscript in preparation). Peptide (b) was synthesized at the University of Texas Molecular Biology Core facilities. *Ets*[42] and PEA-15[28] were expressed and purified as described earlier.

All NMR samples for the binding experiments were prepared in NMR buffer that did not contain Mg^{2+} or ADP. The ERK2 concentration was ~200 μM containing an excess of the specific unlabeled ligand (400 μM Ste-7 peptide, 500 μM Elk-1 peptide, 1 mM *Ets*, and 1 mM PEA-15). For all samples, ^{15}N-, ^{1}H-TROSY-, and TROSY-based HNCO and HNCA (only for the Elk-1 peptide, *Ets*, and PEA-15) experiments were recorded at 700, 800, or 900 MHz. Combined backbone chemical shift changes were evaluated using the formula given below, utilizing the chemical shift perturbations for $^{13}C'^{i-1}$, $^{15}N^{i}$, and amide $^{1}H^{i}$ nuclei from a TROSY-based HNCO experiment (see Supporting Information Table S1):

$$\Delta\delta = \sqrt{(0.46\Delta\delta_{^{13}C',i-1})^2 + (0.17\Delta\delta_{^{15}N^i})^2 + (\Delta\delta_{^{1}H^i})^2}$$

Note that we relied on 3-dimensional TROSY-HNCO spectra in the presence of saturating amounts of ligand rather than on 2-dimensional ^{15}N and ^{1}H TROSY experiments to evaluate chemical shift perturbations. This was necessary due to the extensive spectral overlap that resulted in a limited number of residues that could be analyzed using 2-dimensional spectra. Nevertheless, a representative example of a titration course using 2-dimensional spectra is shown in Figure S1. These spectra illustrate the gradual change in chemical shift values in a ^{15}N and ^{1}H TROSY experiment in the presence of increasing amounts of ligand. Absolute values of the $^{13}C^{\alpha}$ chemical shift perturbations (see Table S2) in the presence of the ligands were also measured using TROSY-based HNCA experiments. All spectra were processed using NMRpipe[43] and analyzed using Sparky (Goddard, T. D., and Kneller, D. G., University of San Francisco). Chemical shifts perturbations were deemed significant if exceeded an internal threshold (around 0.06 ppm for the two D-site peptides and *Ets* and around 0.11 ppm for PEA-15) defined as the average perturbations plus twice the standard deviation calculated on a portion of the protein (typically the first 70 residues) not expected to participate in the binding interaction. To minimize possible perturbations induced by the buffer and temperature changes, the same buffer stock was used for all samples, and all instruments were temperature calibrated using methanol. The pH values of the samples were checked before and after addition of the peptides. It should be noted that the duplicate reference spectra collected at different times and at different spectrometer frequencies were highly superimposable, providing a control for the specific nature of the chemical shifts seen.

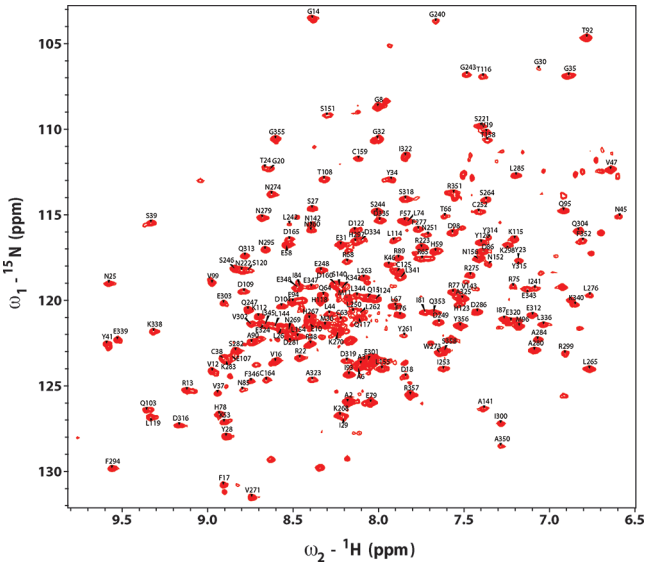

Figure 2. Partially assigned ^{15}N,^{1}H TROSY spectrum of inactive full-length rat ERK2 at 800 MHz. The spectrum was acquired at 25 °C, in a buffer containing 50 mM phosphate, 150 mM NaCl, 2 mM DTT, and 500 μM EDTA at pH 6.8. The spectral parameters were: SW_{1H} 15.0 ppm, 1024 complex points; SW_{15N} 33.0 ppm, 128 complex points, recycling delay 1.5 s, 16 transients were used per t_1 point.

RESULTS

Using available structural information, spin-labeled ATP analogues, selectively labeled samples in addition to conventional backbone-directed resonance assignment strategies, a total of 89.4% of the ^{1}H,^{15}N resonances that were observed at 800 MHz (65.1% of all expected resonances) were unambiguously assigned (see Figure 2). Of the regulatory elements conserved in protein kinases,[10,11] 81% of the regulatory helix αC, 100% of the Gly-rich loop and D165 of the DFG motif were assigned. In addition, assignments were obtained for 62% of the C-spine and 50% of the R-spine (see Figure 1A). However, few assignments could be obtained for the αF helix (16%) and the catalytic and activation loops. The extent of ^{1}H, ^{15}N resonance assignment for the DRS was almost complete (95%) and partially complete for the FRS (46%, excluding the activation loop). The procedures used to achieve this level of resonance assignment for a system such as this is highly nontrivial and will be described at length elsewhere.[41]

Having obtained a significant portion of the resonance assignments at the sites of protein−protein interactions involving

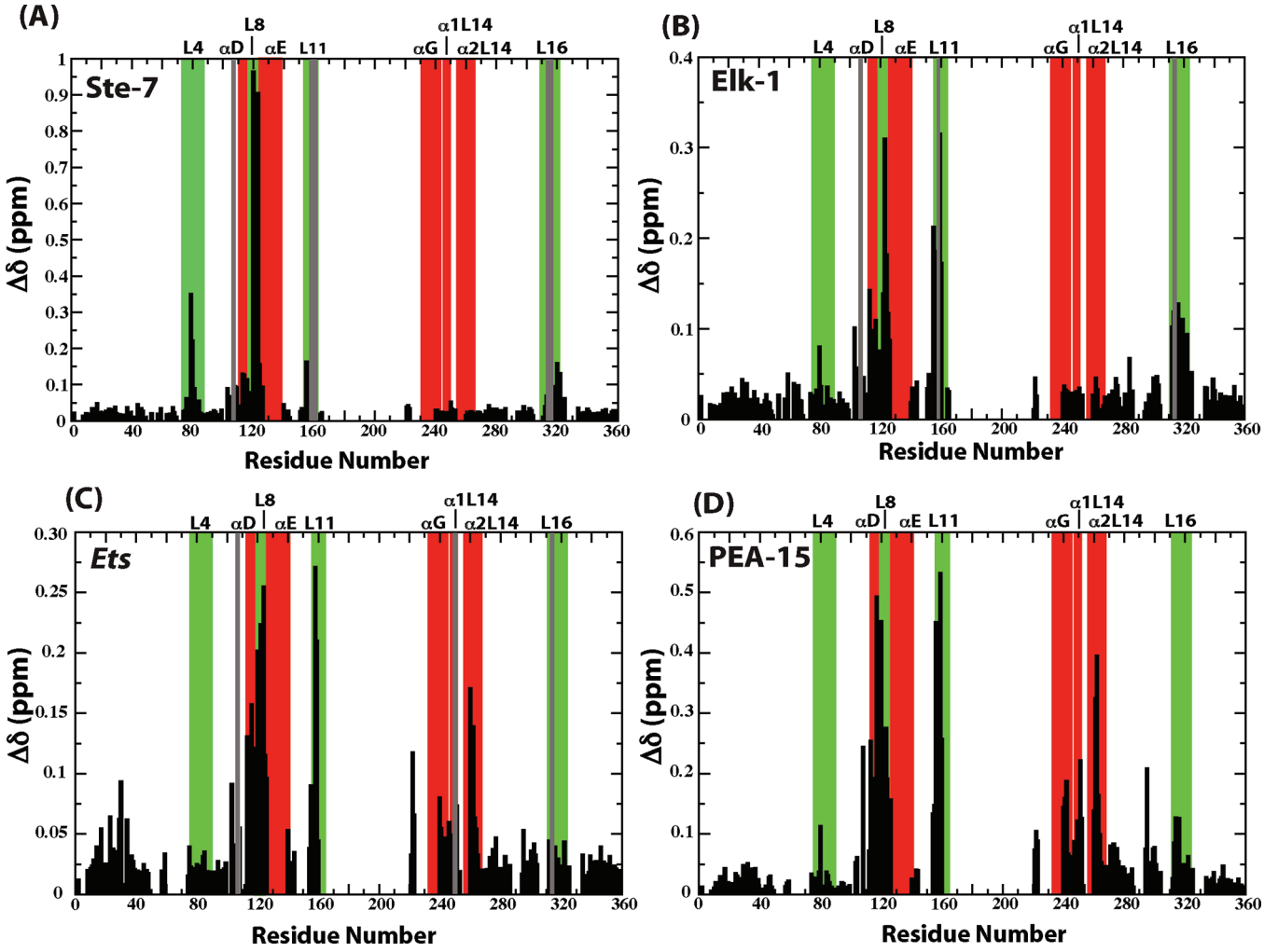

Figure 3. Plots of the combined backbone chemical shift perturbations (calculated from amide ^{15}N, ^{13}CO, and ^{1}H chemical shift changes in TROSY-based HNCO experiments; see Table S1, footnote *b*) induced on inactive ERK2 by (A) a Ste-7-derived peptide, (B) an Elk-1-derived peptide, (C) *Ets*, and (D) full-length PEA-15. Gray bars indicate resonances that disappear upon ligand binding. Also see Table S1 for numerical values of the backbone chemical shift changes. Select helices and loops are shaded red and green, respectively.

ERK2, we focused on determining the chemical shift perturbations reflective of structural changes induced by a series of upstream and downstream regulators and targets that bear both canonical as well as noncanonical binding motifs. See Tables S1 and S2 for numerical values of the chemical shift perturbations.

Binding of a Peptide Derived from the N-Terminus of Ste-7 to Inactive ERK2. The MAPKK Ste-7 has been shown to interact with and phosphorylate Fus3, the yeast ortholog of ERK1/2, and this interaction plays a central role in the MAPK signal cascade that regulates mating signals in yeast.[44] As our first target, we tested the structural perturbations induced by a peptide derived from the N-terminus of Ste-7 fused to a 9-residue substrate motif using three 6-aminohexanoic acid (Δ) spacers: ^{2}FQRKTLQRRNLKGLNLNL^{19}-$(\Delta)_3$-TGPLSPGPF (Ste-7 numbering shown). This conserved N-terminal motif has been shown to be sufficient to bind to ERK1 and ERK2.[45] This peptide contains a canonical D-site sequence ^{9}RRX$_5$^{15}LXL^{17} (where L15 and L17 correspond to the two D-site hydrophobic residues Φ_A and Φ_B, respectively; binding is abolished when these residues are mutated to Ala[45]). As expected, the peptide induces chemical shift perturbations localized in the DRS (see Figures 3A and 4A). In particular, several residues located on loop 16 containing the Φ_{chg} subsite, which include the charged residues D316, D319, and E320, are affected by ligand binding. The Φ_{chg} subsite interacts with the two charged residues, R9 and R10, located at the N-terminus of the D-site sequence. Charge reversal mutations, R9E and R10E, almost completely abolishes binding to ERK2.[45] Perturbations on the Φ_{hyd} subsite (that hosts the hydrophobic Φ_A and Φ_B residues of the D-site) are localized on helix αE, loop 8, helix αD, and loop 11. In this area, a number of hydrophobic residues including L113 and L155 are perturbed. Together with F127, these residues have been proposed to be critical for the recognition of the D-site sequence (F127 is unassigned, however neighboring Y126 is perturbed).[46] Further, perturbations are also observed on loop 4, in the linker connecting the N- and C-lobes and at the end of strand β5 (Q103, the so-called gatekeeper residue; see below).

A superposition of the crystal structure of the Ste-7 peptide bound to Fus3[22] onto the crystal structure of inactive ERK2 bound to a peptide derived from the tyrosine phosphatase HePTP[23] (see Figure 4C) suggests similarities between their binding modes. In the two kinases, i.e. ERK2 and Fus3, the DRS

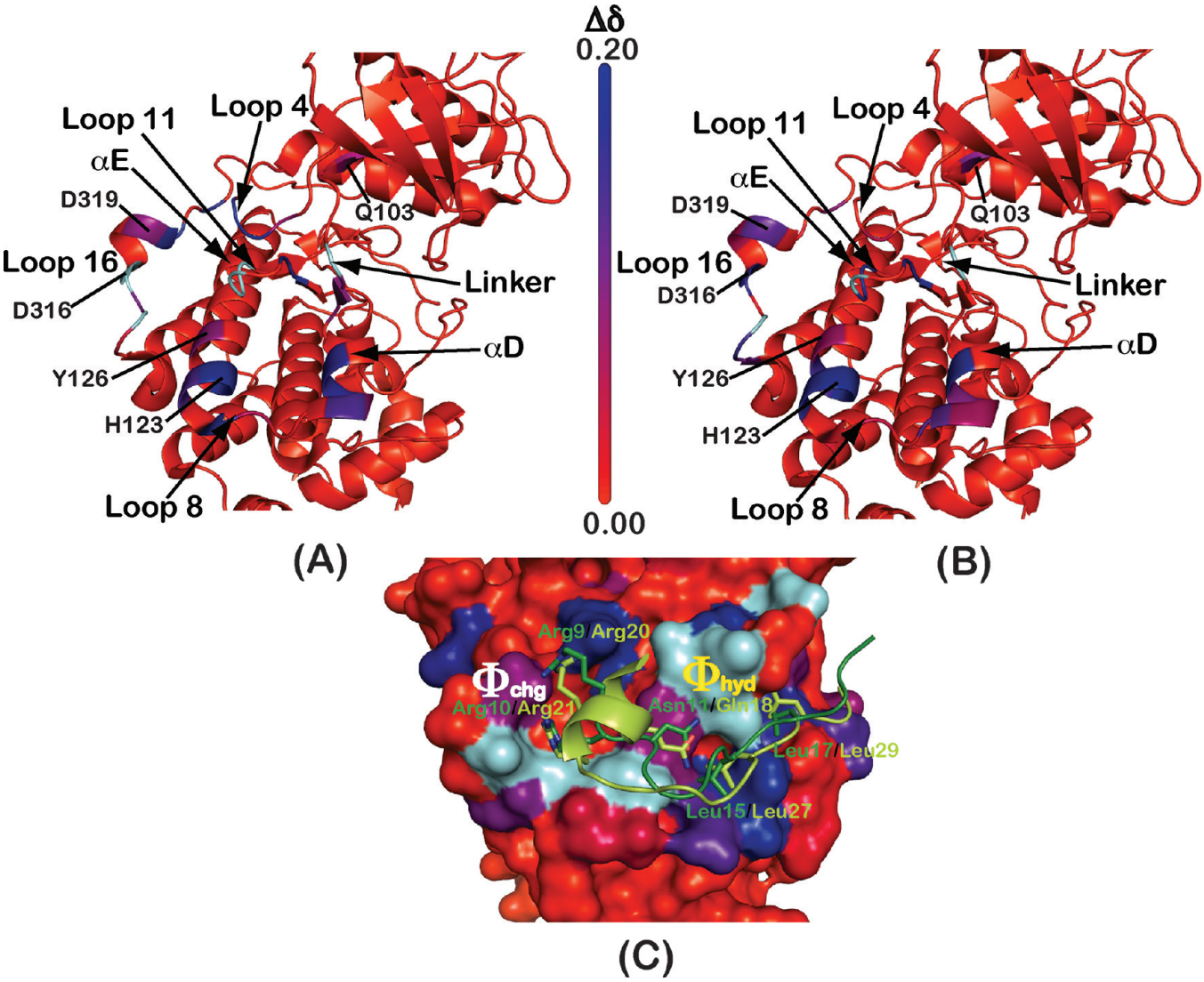

Figure 4. Combined backbone chemical shift perturbations (^{15}N, ^{1}H, and ^{13}C′ from a TROSY-HNCO experiment) induced on ERK2 by a D-site peptide derived from (A) Ste-7 or (B) Elk-1 are plotted on a ribbon representation of inactive ERK2 (PDB ID: 2GPH) using a red−blue gradient. Important structural elements around the binding sites are labeled. Key residues including the conserved common docking D316 and D319 (from the Φ_{chg} subsite) and H123 and Y126 (from the Φ_{hyd} subsite) that form part of the D-recruitment site (DRS) are labeled. The gatekeeper residue (Q103) that is consistently perturbed is also labeled. Residues that disappear upon ligand binding are colored cyan. (C) The ribbon representations for D-site peptides derived from the phosphatase HePTP (light green) bound to ERK2 (light green) as well from Ste-7 (dark green) bound to the yeast ortholog of ERK2, Fus3 (after superposition of Fus3 to ERK2), are shown. Key side chains for the two ligands are also highlighted. The coloring scheme for the ERK2 surface is the same as in (A) and (B). The chemical shift range has been scaled for coloring to ease visualization. Numerical values of the chemical shift changes can be found in Table S1.

appears to be conserved both in sequence and in structure (i.e., upon superposition of the two domains, for residues within 6 Å from Ste-7 we observed 66.6% sequence identity and a heavy-atom rmsd of 0.57 Å) and both ligands appear to adopt a similar overall orientation in the binding pocket. Though the backbone arrangement of the two peptides is only approximately similar (they both share a similar L-shaped topology, with one segment recognizing the Φ_{chg} subsite and the second segment the Φ_{hyd} subsite, with a Asn/Gln residue stabilizing the turn between these two segments), a number of key conserved side chains are spatially coincident, and their orientation is fully consistent with the observed chemical shift perturbations (see Figure 4C). In particular, R9 on Ste-7 (R20 in HePTP) interacts with perturbed D319 on loop 16 and E79 on loop 4; R10 on Ste-7 (R21 in HePTP) interacts with perturbed D316 and E320 on loop 16. L15 on Ste-7 (L27 in HePTP, residue Φ_A from the D-site) interacts with perturbed H123 and Y126, and L17 on Ste-7 (L29 in HePTP, Φ_B) is buried in a pocket including T108, L113, L155, and C159, all of which show significant chemical shift perturbations. The only long-range perturbation observed involves Q103, the gatekeeper residue, which has been suggested to be allosterically coupled to the active site.[47] This, together with the linker perturbations belonging to residues flanking the ATP binding pocket, may explain the modest 1.3-fold change in the k_{cat} for the ERK2-catalyzed phosphorylation of an F-site-derived substrate, observed upon engaging of the DRS by the Ste-7 peptide (Lee et al., in preparation). It has been shown that docking interactions lead to significant conformational changes at the catalytic

dx.doi.org/10.1021/bi2000559 |*Biochemistry* 2011, 50, 3660–3672

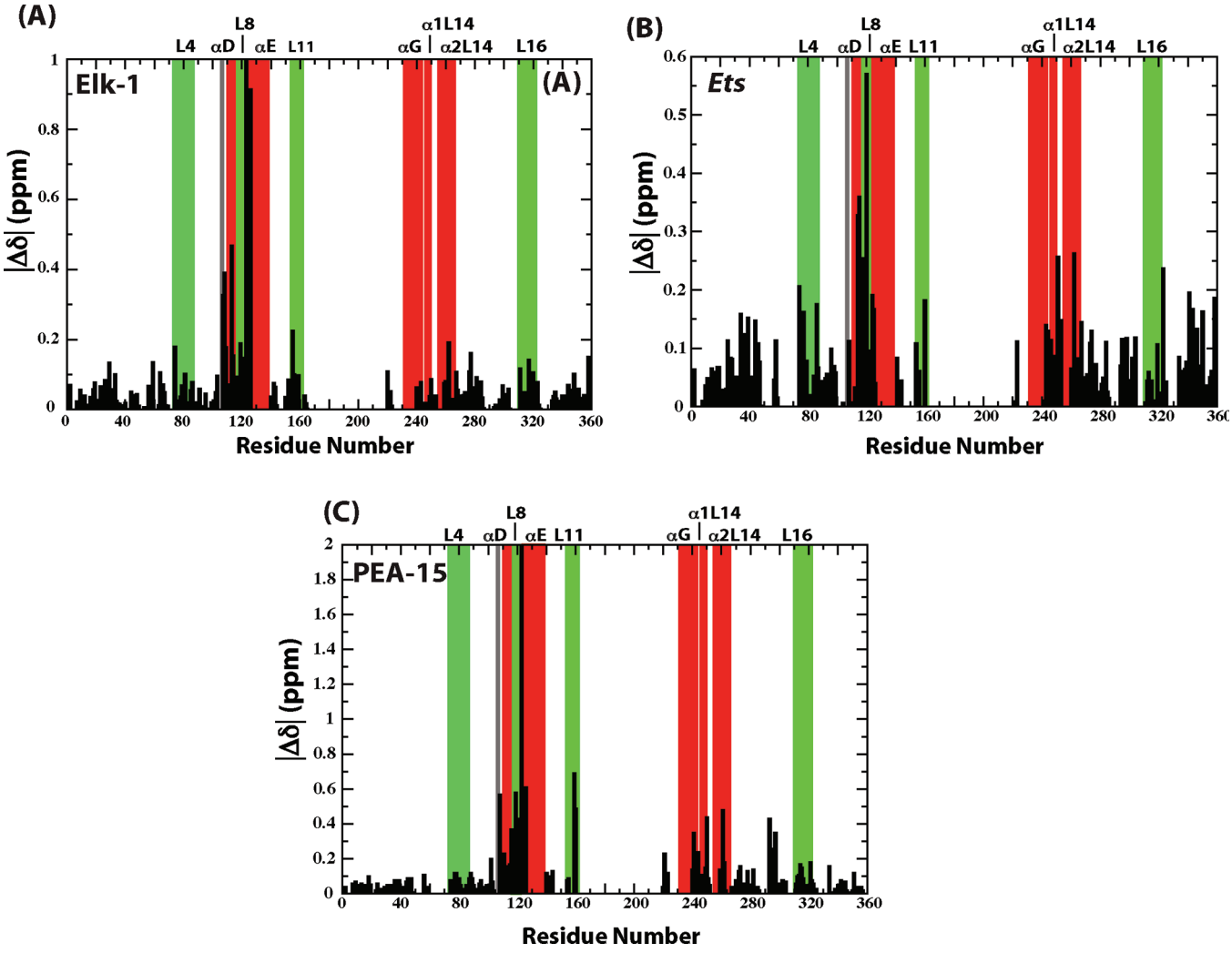

Figure 5. Plots of absolute chemical shift changes for $^{13}C^{\alpha}$ nuclei (obtained using TROSY-based HNCA experiments) induced on inactive ERK2 by (A) an Elk-1-derived peptide, (B) *Ets*, and (C) PEA-15. Note that in (A) and (C) the shifts for H123 (3.4 and 3.75 ppm, respectively) are larger than the ordinate axis window. Also see Table S2 for numerical values of the $^{13}C^{\alpha}$ chemical shift changes.

site and result in an active-like conformation.[24] The C-terminal part of the peptide corresponding to a substrate sequence was not expected to interact with inactive ERK2, and indeed no other perturbations distant from the DRS can been seen in the N-lobe, although the catalytic and activation loops are largely unassigned. No significant perturbations were observed at the FRS.

Binding of a Peptide Derived from Elk-1 to Inactive ERK2. Next we investigated the binding of a D-site peptide derived from the transcription factor Elk-1 (^{311}QKGRKPRDLELPLSPSL^{327} containing the canonical D-site sequence, ^{314}RKX$_5$LXL^{323}), a member of the ETS family,[9] that is a substrate for ERK2.[48,49] This peptide also induces significant chemical shift perturbations in the DRS (see Figures 3B and 4B). Loop 16 (Φ_{chg} subsite) is moderately affected; among others, the acidic residues E312, D316, and D319 display small but significant chemical shift changes. On loop 4 small perturbations are observed for N80, but not for E79. On the Φ_{hyd} subsite, perturbations are localized on helix αE and helix αD; only modest perturbations are seen for loop 8. Again, as in the case of Ste-7, the hydrophobic residues, L113, L155, and Y126 are affected by ligand binding. Perturbations are further observed on loop 11, on the linker between the N- and C-lobes and at the end of strand β5 (Q103). In addition, in the presence of the Elk-1-derived peptide, a TROSY-based HNCA spectrum was also collected, and the deviations of $^{13}C^{\alpha}$ chemical shift from the unbound state, which are particularly sensitive to changes in backbone secondary structure, were computed (see Figure 5A). Here, chemical shift perturbations are localized on helix αE and, to a lesser extent, on helix αD and on the interdomain linker (see Table S2).

The Φ_{chg} subsite perturbations on the common docking residues D316 and D319 indicate that their side chains engage R4 and K5 on the N-terminal end of the Elk-1 peptide; however, the lack of perturbations on E79 and E320 (that display perturbations for the Ste-7 peptide) suggests that the spatial arrangement of the basic residues in Elk-1 is somewhat different from that observed in the known crystal structures of ERK2-bound D-peptides.[23,24] This finding appears to be in contrast to the results of Zhang and co-workers, who reported a modest 1.8-fold increase in the K_M for the E79A mutant.[50] The architecture of loop 4 is well conserved in all ERK2 crystal structures, and the side chain of E79 is part of an electrostatic network involving R133 and the acidic residues on loop 16. It is therefore conceivable that

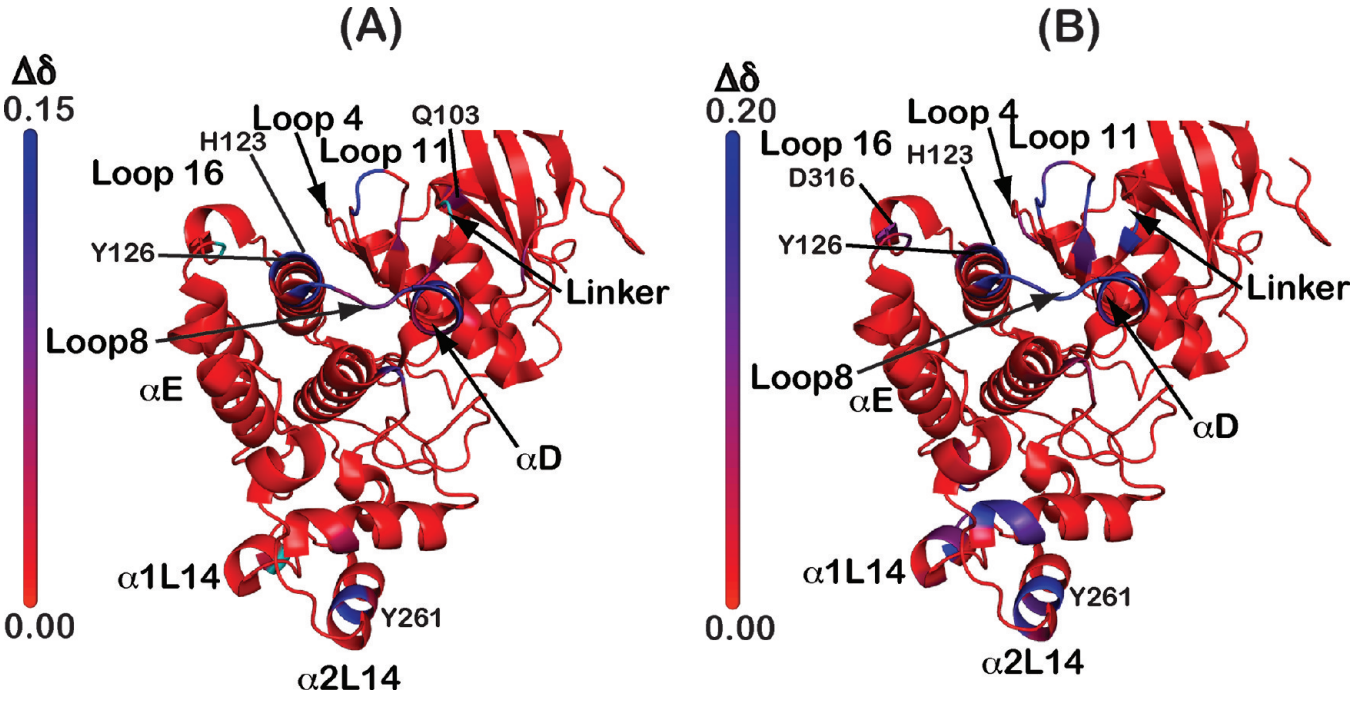

Figure 6. Combined backbone chemical shift perturbations (^{15}N, ^{1}H, and ^{13}C′ from a TROSY-HNCO experiment) induced by (A) *Ets* and (B) full-length PEA-15 are plotted on a ribbon representation of ERK2. Key residues are labeled as in Figure 4. Also labeled is the perturbed residue Y261 that has been suggested to form a part of the FRS from HXMS studies.[21] The chemical shift range has been scaled for coloring to ease visualization. Actual shift changes can be found in Table S1.

the E79A mutation indirectly affects the K_M by somewhat altering the overall conformation of the kinase. The 3-fold decrease in k_{cat} associated with the E79A mutant[50] would also be consistent with this scenario. The chemical shift perturbations observed for the backbone amide resonances of the hydrophobic residues of helices αE, αD and loop 11 indicate that the interaction of L320 (Φ_A) and L322 (Φ_B) from the Elk-1 peptide with these hydrophobic clefts represents the other major determinant for Elk-1 binding.

In general, the very limited number of $^{13}C^{\alpha}$ perturbations (see Figure 5A) detected for ERK2 in the presence of Elk-1 confirms that the overall backbone architecture of the DRS does not change upon peptide binding. Interestingly, however, the only significant changes in the $^{13}C^{\alpha}$ chemical shifts were also found in this area (H123 and Y126). This indicates that the insertion of the hydrophobic side chains from Elk-1 into the protein core does slightly affect the local conformation. In the crystal structures of ERK2 bound to peptidic ligands, the αE helix does not seem to undergo any significant conformational changes. It is however tempting to interpret the significant downfield shifts of the $^{13}C^{\alpha}$ resonances for H123 and Y126 as a consequence of an increased rigidity of the αE helix induced by the peptide binding. The remaining $^{13}C^{\alpha}$ perturbations are found on the linker between the N- and C-lobes. These perturbations, combined with those seen for the backbone amide resonances for β5, indicate that binding of the Elk-1 peptide may alter the relative orientation of the N- and C-lobes. Lack of perturbations on or near the FRS confirmed the results obtained for the Ste-7 case and indicated that binding to the DRS by canonical D-site ligands does not have any significant effects on the FRS.

It is to be noted that a hydrogen exchange mass spectrometry (HXMS) study is available on the same peptide with active ERK2.[21] These results indicate the highest levels of protection for the αD and αE helices and loop 11 in the presence of the Elk-1 peptide, in line with the nature of chemical shift perturbations seen here. Loop 16 bearing the Asp residues of the common docking motif whose chemical shifts are perturbed also experiences increased protection. Interestingly, loop 4 (as reported by N80) that displays small chemical shift perturbations experienced decreased protection in the HXMS studies. The incompleteness of resonance assignment in the activation and catalytic loops prevented a comparison for this region. Overall the NMR and HXMS results are in agreement though some minor incongruities could be the result of differences between active (used in the HXMS studies) and inactive (used in the present study) ERK2.

Interactions of Ets-1 with Inactive ERK2. Having analyzed the structural perturbations induced by canonical D-site peptides, we focused our attention toward investigating the structural perturbations resulting from Ets-1 that belongs to the ETS family of transcription factors.[9] Ets-1 is phosphorylated by ERK2 on T38 that lies on a consensus (ΦXS/TP, Φ is a hydrophobic residue) sequence. This residue lies in a disordered region at the N-terminal end of the α-helical pointed (PNT) (or SAM) domain of Ets-1[51]. Ets-1 binds both active ERK2 and inactive ERK2, the latter believed to be incapable of fully recognizing the ^{36}LXTP^{39} sequence,[27] with comparable affinity. An overall similarity between the binding modes of Ets-1 on both the active and inactive forms of the enzyme has been suggested.[15,52] Interestingly, Ets-1 does not possess any canonical D- or F-sites and yet can be displaced by the D-site peptide from Elk-1 (discussed above) from inactive ERK2.[27] This suggests that Ets-1 utilizes the DRS to interact with inactive ERK2. Additionally, involvement of the FRS in Ets-1/ERK2 interactions has also been noted.[27]

Binding of a construct consisting of the 138 N-terminal residues of Ets-1 (Ets-1Δ138, referred to as *Ets* for simplicity) to inactive ERK2 induces a number of perturbations on the surface of the latter (see Figures 3C and 6A). A majority of these perturbations are localized on the Φ_{hyd} subsite of the DRS (helix αE, αD, loop 8 and on loop 11) and again includes L113, L155, and Y126 (as in the case of the canonical D-site peptides from Elk-1 and Ste-7). No significant perturbations are observed on the charged residues on the Φ_{chg} subsite or on loop 4. Other perturbations contiguous to the DRS are found on helix αF (N222) and on the N- to C-lobe linker. Long-range amide perturbations on the N-lobe are observed on strands β1 (G30) and β5 (Q103). Unlike in the case of the canonical D-site peptides, a second set of perturbations for main-chain amides are seen at the FRS on helix α2L14 in the MAPK insert and on helix αG. Most notably, significant perturbations are seen for Y261 and its flanking residues. This residue has been shown to be crucial in binding canonical F-site peptides and is a crucial component of the FRS.[21] On the MAPK insert, the disappearance of the resonance corresponding to L250 on helix α1L14, which is not part of the canonical FRS site (see Figure 1 and Figure S2), was observed. It should be noted that assignments are not available for all residues that constitute the FRS (see Figure S2); however, a large number of FRS residues for which assignments are available do show chemical shift changes (see Figures 3C and 6A and Figure S2) in the presence of *Ets*. As discussed earlier, no resonance assignments are available for the part of helix αG that bears the residues Y231 and L232 (see Figure S2) that have also been shown to be involved in formation of the FRS.[21] However, cysteine footprinting studies reveal that position 232 shows a 3.5-fold higher protection against cysteine alkylation in the presence of *Ets* than in its absence (see Figure S3). This, in combination with our NMR results, suggests that a large part of the FRS is indeed involved in recognizing *Ets*. The magnitude of the $^{13}C^{\alpha}$ perturbations (see Figure 5B) is reduced compared to that seen for the Elk-1 peptide (however, H123 that undergoes the largest shift in the $^{13}C^{\alpha}$ resonance position in the case of the Elk-1 peptide was severely broadened and could not be assigned in the presence of *Ets*). Most of the $^{13}C^{\alpha}$ perturbations are seen on loop 8 and on helix αD, weak perturbations are also localized on the MAPK insert (see Table S2).

The NMR data indicate that *Ets* binding to inactive ERK2 involves both the DRS and at least part of the FRS. This is consistent with the proposed binding model for active ERK2 where *Ets* engages the ERK2 DRS using its flexible N-terminal extension, and the PNT domain recognizes a binding pocket (part of the FRS) composed of α2L14 on the MAPK insert, the αG helix, and the end of the activation loop[15,52] (also see Figure S4). Indeed, an Ets-1 construct consisting of only the PNT domain (residues 51−138) binds ERK2 with a 20-fold reduced affinity, and a construct that contains only the flexible N-terminus (residues 1−52) binds ERK2 with a 4-fold reduced affinity.[15] Site-directed mutations in the PNT domain also implicate it in interactions with ERK2.[53] The lack of perturbations on the Φ_{chg} subsite as well as on loop 4 indicates that electrostatic interactions, typically involving basic residues on the N-terminal portion of the DRS binding peptide, do not play an appreciable role here. Our data suggest that hydrophobic interactions at the Φ_{hyd} subsite are primarily responsible for the binding of *Ets* at the DRS. The extent of the perturbations, involving helix αE, αD loop 8, and loop 11, indicates that the hydrophobic pocket is fully recognized, which normally requires at least two hydrophobic side chains from the ligand. Modeling studies (see Figure S4, ref 52) suggest that three hydrophobic residues from the flexible N-terminal extension of *Ets*, namely L11, I13, and I14, may engage the Φ_{hyd} subsite of the DRS. Interestingly, a mutation of the αE residue H123 (at the Φ_{hyd} subsite) to Ala leads to the largest increase in K_M for *Ets* phosphorylation by ERK2, whereas the double mutation D316A/D319A (common docking Asp residues on Φ_{chg}) had little effect on K_M.[29] On the *Ets* side, L11 that is suggested to occupy the pocket generated by H123 and Y126 (usually occupied by Φ_A residue on a canonical D-site) on ERK2 when mutated to Asp leads to a 3-fold increase in K_M with no observation change in k_{cat}.[52] A I13D/I14D double mutation leads to similar effects suggesting a role for these hydrophobic residues in the *Ets*/ERK2 interaction.

Chemical shift perturbations of the main-chain amides at the FRS, previously undetected for the D-site ligands, indicate that this site, which is remote from the DRS, is also involved in the *Ets* recognition process. The relatively modest $^{13}C^{\alpha}$ perturbations show that *Ets* binding does not introduce large structural changes in the kinase, with some local structural rearrangement localized on the Φ_{hyd} subsite. Chemical shift perturbations on the linker between the N- and C-lobe and for the N-lobe itself are indicative of some long-range effects, but they do not differ significantly from those induced by the D-site ligands discussed above.

Binding of Full-Length PEA-15 to Inactive ERK2. The adaptor protein PEA-15 has been shown to regulate the cellular localization of ERK2. It has been shown to associate specifically with ERK2 but not the homologous MAPK p38, blocking ERK2-dependent transcription by preventing its translocation to the nucleus.[54] PEA-15 has an all α-helical death-effector domain fold (DED) with a disordered C-terminus.[55] NMR and mutational analyses have revealed a direct and specific interaction of inactive ERK2 with PEA-15 involving both the C-terminus and the DED of the latter.[55] The C-terminus has been predicted to bind the DRS of ERK2.[28] It is therefore only logical to investigate the structural perturbations induced by PEA-15 on ERK2 using NMR chemical shift mapping. The overall pattern of chemical shift perturbations seen is similar in location to that observed for *Ets* (see Figures 4D and 6B), although the magnitude of the perturbations is greater by a factor of around 2. As in *Ets*, loop 16 is poorly perturbed, with the only noticeable difference being the perturbation of the common docking D316, in addition to Y314, though these perturbations are quite small in comparison to others seen in the presence of PEA-15. A weak but detectable perturbation is also found for N80 on loop 4. Again, the largest variations are localized on helix αE, on helix αD, on loop 8, and on loop 11. Perturbations are also found at the end of helix αF and on the N- to C-lobe linker. At the FRS, all segments for which resonance assignments are available, including portions of helix αG as well as helix α2L14 (including Y261), exhibit appreciable perturbations. However, in contrast to *Ets*, PEA-15 also induces strong perturbations on helix α1L14 (see Figure 6).

As in the case of the Elk-1 peptide, the largest perturbations in $^{13}C^{\alpha}$ chemical shifts (see Figure 5C) are seen for H123 and Y126 on αE, but in this case, detectable $^{13}C^{\alpha}$ perturbations are widespread on the DRS (loop 11, helix αD, and loop 8) and on the MAPK insert (helices α2L14 and α1L14).

In contrast to *Ets*, the perturbations detected for D316 and loop 4 suggest an involvement of electrostatic interactions in stabilizing the ligand at the DRS site. However, these perturbations are few and weak, and therefore, as is the case for *Ets*, it seems that PEA-15 mainly recognizes the DRS through

hydrophobic interactions involving the Φ_{hyd} subsite. As mentioned in the case of *Ets* earlier, these interactions are likely to require at least two hydrophobic side chains (as in *Ets* discussed earlier) of the ligand. On the basis of the data of Hill et al.,[55] we hypothesize that these are likely to be I121 and L123. Mutation of these residues abolishes the PEA-15/ERK2 interaction *in vitro* and also suppresses ERK2-dependent transcriptional activity *in vivo*.[55]

The influence of several FRS residues of ERK2 on PEA-15 binding has been assessed through extensive site-directed mutagenesis. Most notably, the mutations K257E and R259E[14] (for which assignments are not available but lie in close proximity to Y261 and L262 which show extremely large perturbations; see Table S1) greatly reduced PEA-15 binding. All of these residues lie on α2L14, suggesting its direct role in recognizing PEA-15. In addition, K229 and Y231 (on αG, for which assignments are not available) also seem to play a substantial role in PEA-15 binding.[14] This role is confirmed by the 110-fold greater protection from Cys alkylation at position 232 in the presence of PEA-15.[28] Large chemical perturbations are also seen in helix α1L14 (see Table S1 and Figure S2) that is not considered to be a part of the FRS. Mutation of N251 (that also shows significant chemical shift perturbations) does not significantly affect PEA-15 binding.[14] Though additional mutational data are required to confirm its role, it seems that α1L14 likely plays an indirect role in PEA-15 binding.

From $^{13}C^{\alpha}$ perturbations, it appears that PEA-15 affects the local conformation of ERK2 more than any other ligand examined by us so far. As seen for the Elk-1-derived peptide, the largest $^{13}C^{\alpha}$ perturbations are located at the Φ_{hyd} subsite (see Figure 5C), and especially for H123 and Y126, but several other perturbations can be found at the FRS and on several flexible regions, including the N- to C-lobe linker. This suggests substantial local conformational rearrangements in ERK2 upon interactions with PEA-15.

DISCUSSION

Docking interactions represent a key mechanism to affect cellular signaling involving MAP kinases, as they mediate the formation of regulatory complexes and modulate the specificity and the efficiency of all the catalytic processes involving up-regulating kinases, down-regulating phosphatases, and downstream substrates.[17] Among the large number of substrates and regulatory proteins targeting the ERK2 docking sites, there are currently only two crystal structures that illustrate docking interactions involving ERK2, and in both cases ERK2 is bound at the DRS to peptides derived from protein phosphatases, namely HePTP[24] and MKP3.[23] While no direct crystallographic information is available for an F-site ligand bound at the FRS, HXMS data coupled with site-directed mutagenesis have provided insight into the nature of this site and key residues that constitute it.[21] For interactions that do not employ canonical D-site or F-site sequences, a number of studies have already appeared in literature aimed at mapping the ERK2 binding surfaces using biochemical techniques[15,27−29] though no direct structural information exists. These studies involve the use of site directed mutagenesis to evaluate the role of a particular residue in ligand binding (K_M or K_D) or in kinetic efficiency (k_{cat}/K_M). Another approach that has been used to examine ERK2 utilizes cysteine footprinting, where a cysteine mutation is inserted into the surface of interest, and its rate of alkylation is measured in the presence and absence of ligands.[29] Unlike the techniques described above, NMR is a biophysical method that allows comprehensive monitoring of the effects of ligand binding on the entire protein, without the need to mutate, or chemically modify the interacting partners. For the present study we have utilized two peptide ligands derived from Ste-7 (a yeast ortholog of the up-regulating MAPKK) and from Elk-1 (an ERK2 substrate), both binding inactive ERK2 in the micromolar range[27] and both bearing canonical MAPK docking motifs (D-sites). The role of noncanonical interactions involving ERK2 has also been tested utilizing an N-terminal construct from an ERK2 substrate the transcription factor Ets-1 and the antiapoptotic adaptor protein PEA-15, both of which bind inactive ERK2 with micromolar affinity. Our studies not only demonstrate the feasibility of investigating docking interactions involving a full-length ERK/MAP kinase using solution NMR methodology but also provide considerable insight into the nature of these interactions including those for which no direct structural evidence is available.

Comparing different ligands that employ the D-site allows a clearer understanding of the recognition mechanism employed by the DRS. We find that for canonical D-site interactions each particular ligand induces a discrete sets of chemical shift perturbations on the DRS surface, which suggests that the DRS surface is quite rigid. If it were not, a more uniform distribution of the perturbations across the DRS would be observed upon ligand binding. This overall rigidity and lack of any major changes in backbone conformation is also borne out by the limited number of $^{13}C^{\alpha}$ chemical shift perturbations seen in this region. On the other hand, this observation indicates that the DRS is also promiscuous, seemingly employing slightly different recognition modes for the two D-site ligands tested, and this is particularly evident at the Φ_{chg} subsite. For example, as pointed out earlier, the binding mode of the Ste-7 peptide appears to be similar to that observed for the Ste-7/Fus3 crystal structure[22] and involves a number of charged residues on loops 4 and 16. The Elk-1 peptide, on the other hand, also engages the Φ_{chg} subsite, but some of the perturbations observed for Ste-7 (for instance, E320 on loop 16 or E79 on loop 4) are not seen, indicating a different pattern of electrostatic interactions (note that there are no crystal structures of ERK2 in complex with either the Elk-1 or Ste-7 peptides). Elucidation of these residue-by-residue differences is a unique strength of atomistic techniques such as NMR and cannot be easily obtained from fragment-based approaches such as HXMS.

In contrast to the Φ_{chg} subsite, the Φ_{hyd} subsite reveals large chemical shift perturbations in both the canonical (Ste-7, Elk-1) as well as the noncanonical (Ets-1, PEA-15) cases. These perturbations are consistently localized on helix αE, helix αD, and loop 11. This is also where $^{13}C^{\alpha}$ perturbations can primarily be found. Our data are consistent with the idea that the Φ_{chg} subsite interactions consist of electrostatic contacts originating from charge−charge interactions between side chains located on the protein surface and have little effect on backbone architecture. The interactions hosted by the Φ_{hyd} subsite, on the other hand, involve the insertion of hydrophobic side chains of the ligand into the hydrophobic core of the protein and therefore likely induce significant conformational changes in the affected area, including the backbone. Interestingly, the loop 16 residue Y314, whose side chain is positioned between the two subsites, is also consistently perturbed. Some variation in the pattern of chemical shift perturbations can also be found at the Φ_{hyd} subsite. For instance, L155 (loop 11) is poorly perturbed in *Ets* with respect to the other ligands; the $^{13}C^{\alpha}$ chemical shift of Y126

(helix αE) does not undergo major changes in the presence of *Ets*, as found for the Elk-1 peptide and PEA-15; K115 (loop 8) does not seem to be affected by PEA-15 binding but displays significant perturbations in all other cases. Thus, it appears that the DRS can accommodate both canonical and noncanonical ligands mostly through the Φ_{hyd} subsite. Therefore, this site should likely be the target of universal inhibitors of the docking interactions that target the DRS. Given the nature of residues in the disordered ends of *Ets* (N-terminal) and PEA-15 (C-terminal) that are suggested to engage the Φ_{hyd} subsite, it can be speculated that the hydrophobic residues (L11, I13/I14 on *Ets* and I121, L123 on PEA-15) may perhaps substitute for the hydrophobic part, i.e., $\Phi_A-X-\Phi_B$ of a canonical D-site.

Interactions involving the Φ_{chg} subsite, on the other hand, do not seem to be a strict requirement for the noncanonical ligands that also utilize the DRS. *Ets* interacts poorly with this subsite, inducing no perturbations for the two common docking Asp residues in ERK2. Only a weak perturbation can be found on D316 in the presence of PEA-15. Thus, small molecule inhibitors designed to disrupt interactions involving the Φ_{chg} site are likely to be more effective against ligands that employ canonical D-site sequences that more effectively use the Φ_{chg} region. Interestingly, a mutational analysis indicates that the basic residues on the C-terminal tail of PEA-15 (K128, K129) are necessary for binding.[55] However, the present studies seem to suggest that these charge interactions are less likely to involve the Φ_{chg} region of the DRS. It is also conceivable, however, as noted above, that these interactions primarily involving side-chain moieties are weak enough to only mildly perturb the backbone.

For all ligands tested, in addition to the involvement of the DRS, we consistently detected perturbations on the linker between the N- and C-lobes and on the β5 strand, which constitutes part of the ATP binding pocket. This suggests a slight change in the overall orientation between the two lobes along with a remodeling of the catalytic site. The role of interlobe communications and relative orientation between the N- and C-lobes upon interactions involving the DRS in activation of MAP kinases has been demonstrated in the homologous Fus3 and JNK1 kinases upon docking interactions with Ste-5[56] and Jip1,[57] respectively. For ERK2 as well, the flexibility of the linker and the change of the relative orientation of the N- and C-lobes upon activation have been demonstrated by HXMS studies.[58] In all the cases we analyzed (except for PEA-15) in the present study, Q103, the gatekeeper residue that lies on the β5 strand, is consistently perturbed upon binding of the substrates. Mutation of this residue to Ala or Gly leads to weak constitutive activation of ERK2 through intramolecular autophosphorylation, suggesting that this residue is dynamically coupled to the active site.[47] This information coupled with our current results is suggestive of an allosteric network involving the DRS and the active site, coupled through the gatekeeper. Importantly, we did not observe any effects on the FRS upon binding of the two D-site ligands that specifically target the DRS, suggesting that these two recruitment sites are uncoupled from each other.

In contrast to the D-site peptides, *Ets* and PEA-15 also induce perturbations on a second binding pocket formed by the MAPK insert and helix αG. Therefore, these data support our previously proposed model[15,52] where both *Ets* and PEA-15 bind ERK2 in a bidentate fashion, the folded domain (PNT and DED, respectively) recognizes the FRS, and the flexible extension folds around the ERK2 surface and bind the DRS[15] (also see Figure S4, ref 52). The overall pattern of chemical shift perturbations observed in inactive ERK2 upon binding of both *Ets* and PEA-15 is strikingly similar though larger chemical shift perturbations are seen for PEA-15 than *Ets*. In particular for PEA-15, larger and more extensive perturbations are observed for helix αG and also for the MAPK insert where the perturbations involve both helices α1L14 and α2L14. This may suggest a slight difference in the modes with which PEA-15 and *Ets* engage ERK2 and/or these ligands induce unique conformational changes in ERK2. It should be noticed that, for active ERK2, although *Ets* is displaced by peptides that bind the F-site, PEA-15 is not,[27,28] which would be consistent with our hypothesis.

CONCLUSIONS

The studies presented here represent a first step in utilizing the range of information that solution state NMR spectroscopy can provide for interactions involving ERK/MAP kinases. Our present analysis, based on chemical shift perturbations on inactive ERK2 induced by a range of ligands that employ canonical and noncanonical docking motifs, highlights the similarities and differences between these interactions. Canonical D-site peptides rely on both charge−charge and hydrophobic interactions to dock onto ERK2. Noncanonical ligands such as Ets-1 and PEA-15 primarily utilize hydrophobic interactions. These findings are in agreement with mutational and functional studies and also with results from HXMS studies, where available. We also confirmed the results of prior biochemical and mutational studies that the aforementioned noncanonical ligands utilize two distinct docking sites for ERK2 recognition, probably as a way to achieve higher selectivity (in the case of a substrate like Ets-1) or more effective inhibition (in the case of the regulator PEA-15). Our work seems to indicate that these docking sites are not allosterically coupled and are targeted independently by the ligands through two distinct binding motifs.

During the preparation of this manuscript, an initial NMR analysis of D-site interactions in the MAPK p38α appeared in the literature.[34] This study employed a single D-site peptide derived from MEK3b and utilized 133 backbone amide chemical shifts of p38α (that could be transferred from the original assignments of Vogtherr et al.[33] and represent 37% coverage) as probes of structural changes upon binding. The results of that study are in general consistent with our results for the D-site peptides. However, only when multiple D-site ligands are employed, as in the present work, the subtle differences characterizing the modes of D-site peptide recognition by ERK/MAP kinases become evident. Nevertheless, it would be extremely useful to obtain further dynamic and structural details of D-site interactions involving both the ERK and the p38 subfamilies and perhaps others such as the JNKs.[59] As far as noncanonical interactions are concerned, these have been characterized biochemically to a larger extent in ERK2, so at this stage ERK2 represents a more fruitful target for NMR and other biophysical studies.

ASSOCIATED CONTENT

Supporting Information. Representative titration series for ERK2 in the presence of ligand; close-up view of chemical shift perturbations and availability of resonance assignments at the FRS in inactive ERK2; cysteine footprinting studies on ERK2 (L232C) in the presence and absence of *Ets*; a computational model for a complex of *Ets* with active ERK2. This material is available free of charge via the Internet at http://pubs.acs.org.

AUTHOR INFORMATION

Corresponding Author

*Fax (212) 650 6107, phone (212) 650 6049, e-mail rghose@sci.ccny.cuny.edu (R.G.); Fax (512) 232 2606, phone (512) 471 9267, e-mail kinases@me.com (K.N.D.).

Funding Sources

This research has been supported by the following grants from the National Institutes of Health: GM084278 (to R.G.), GM059802 (to K.N.D.), GM079686 (to P.R.), and 5G12 RR03060 (toward partial support of the NMR facilities at The City College of New York). R.G. is a member of the New York Structural Biology Center, NYSTAR facility. K.N.D. is a recipient of a grant from the Welch Foundation (F-1390). Computing resources were provided by TeraGrid (MCB100057).

ACKNOWLEDGMENT

The authors thank Dr. Pia D. Vogel, Southern Methodist University, for a kind gift of the sl-ATP. The authors also thank Dr. Mark Girvin (Albert Einstein College of Medicine) for useful discussions.

ABBREVIATIONS

MAP kinase, mitogen-activated protein kinase; DRS, D-recruitment site; ERK, extracellular signal regulated kinase; DEF, docking site for ERK FXFP; DTT, dithiothreitol; EDTA, ethylenediaminetetraacetic acid; *Ets*, a construct of Ets-1 containing the N-terminal 138 residues; FRS, F-recruitment site; HXMS, hydrogen exchange mass spectroscopy; IPTG, isopropyl β-D-thiogalactopyranoside; MAPKK, mitogen-activated protein kinase kinase; PEA-15, phosphoprotein enriched in astrocytes 15 kDa.

REFERENCES

(1) Murphy, L. O., and Blenis, J. (2006) MAPK signal specificity: the right place at the right time. *Trends Biochem. Sci. 31*, 268–275.

(2) Chen, Z., Gibson, T. B., Robinson, F., Silvestro, L., Pearson, G., Xu, B., Wright, A., Vanderbilt, C., and Cobb, M. H. (2001) MAP kinases. *Chem. Rev. 101*, 2449–2476.

(3) Pearson, G., Robinson, F., Beers Gibson, T., Xu, B. E., Karandikar, M., Berman, K., and Cobb, M. H. (2001) Mitogen-activated protein (MAP) kinase pathways: regulation and physiological functions. *Endocrine Rev. 22*, 153–183.

(4) Fang, J. Y., and Richardson, B. C. (2005) The MAPK signalling pathways and colorectal cancer. *Lancet Oncol. 6*, 322–327.

(5) Kohno, M., and Pouyssegur, J. (2006) Targeting the ERK signaling pathway in cancer therapy. *Ann. Med. 38*, 200–211.

(6) Kohno, M., and Pouyssegur, J. (2003) Pharmacological inhibitors of the ERK signaling pathway: application as anticancer drugs. *Prog. Cell Cycle Res. 5*, 219–224.

(7) Dalby, K. N., Morrice, N., Caudwell, F. B., Avruch, J., and Cohen, P. (1998) Identification of regulatory phosphorylation sites in mitogen-activated protein kinase (MAPK)-activated protein kinase-1a/p90rsk that are inducible by MAPK. *J. Biol. Chem. 273*, 1496–1505.

(8) Roux, P. P., and Blenis, J. (2004) ERK and p38 MAPK-activated protein kinases: a family of protein kinases with diverse biological functions. *Microbiol. Mol. Biol. Rev. 68*, 320–344.

(9) Sharrocks, A. D. (2001) The ETS-domain transcription factor family. *Nat. Rev. Mol. Cell Biol. 2*, 827–837.

(10) Kornev, A. P., and Taylor, S. S. (2010) Defining the conserved internal architecture of a protein kinase. *Biochim. Biophys. Acta 1804*, 440–444.

(11) Taylor, S. S., and Kornev, A. P. (2011) Protein kinases: evolution of dynamic regulatory proteins. *Trends Biochem. Sci. 36*, 65–77.

(12) Parsons, S. J., and Parsons, J. T. (2004) Src family kinases, key regulators of signal transduction. *Oncogene 23*, 7906–7909.

(13) Robinson, F. L., Whitehurst, A. W., Raman, M., and Cobb, M. H. (2002) Identification of novel point mutations in ERK2 that selectively disrupt binding to MEK1. *J. Biol. Chem. 277*, 14844–14852.

(14) Chou, F. L., Hill, J. M., Hsieh, J. C., Pouyssegur, J., Brunet, A., Glading, A., Uberall, F., Ramos, J. W., Werner, M. H., and Ginsberg, M. H. (2003) PEA-15 binding to ERK1/2 MAPKs is required for its modulation of integrin activation. *J. Biol. Chem. 278*, 52587–52597.

(15) Callaway, K., Waas, W. F., Rainey, M. A., Ren, P., and Dalby, K. N. (2010) Phosphorylation of the transcription factor Ets-1 by ERK2: rapid dissociation of ADP and phospho-Ets-1. *Biochemistry 49*, 3619–3630.

(16) Sharrocks, A. D., Yang, S. H., and Galanis, A. (2000) Docking domains and substrate-specificity determination for MAP kinases. *Trends Biochem. Sci. 25*, 448–453.

(17) Remenyi, A., Good, M. C., and Lim, W. A. (2006) Docking interactions in protein kinase and phosphatase networks. *Curr. Opin. Struct. Biol. 16*, 676–685.

(18) Gavin, A. C., and Nebreda, A. R. (1999) A MAP kinase docking site is required for phosphorylation and activation of p90(rsk)/MAPKAP kinase-1. *Curr. Biol. 9*, 281–284.

(19) Akella, R., Moon, T. M., and Goldsmith, E. J. (2008) Unique MAP Kinase binding sites. *Biochim. Biophys. Acta 1784*, 48–55.

(20) Tanoue, T., Adachi, M., Moriguchi, T., and Nishida, E. (2000) A conserved docking motif in MAP kinases common to substrates, activators and regulators. *Nat. Cell Biol. 2*, 110–116.

(21) Lee, T., Hoofnagle, A. N., Kabuyama, Y., Stroud, J., Min, X., Goldsmith, E. J., Chen, L., Resing, K. A., and Ahn, N. G. (2004) Docking motif interactions in MAP kinases revealed by hydrogen exchange mass spectrometry. *Mol. Cell 14*, 43–55.

(22) Remenyi, A., Good, M. C., Bhattacharyya, R. P., and Lim, W. A. (2005) The role of docking interactions in mediating signaling input, output, and discrimination in the yeast MAPK network. *Mol. Cell 20*, 951–962.

(23) Liu, T., Sun, L., Humphreys, J., and Goldsmith, E. J. (2006) Structural basis of docking interactions between ERK2 and MAP kinase phosphatase 3. *Proc. Natl. Acad. Sci. U.S.A. 103*, 5326–5331.

(24) Zhou, T., Sun, L., Humphreys, J., and Goldsmith, E. J. (2006) Docking interactions induce exposure of activation loop in the MAP kinase ERK2. *Structure 14*, 1011–1019.

(25) Shi, Z., Resing, K. A., and Ahn, N. G. (2006) Networks for the allosteric control of protein kinases. *Curr. Opin. Struct. Biol. 16*, 686–692.

(26) Sheridan, D. L., Kong, Y., Parker, S. A., Dalby, K. N., and Turk, B. E. (2008) Substrate discrimination among mitogen-activated protein kinases through distinct docking sequence motifs. *J. Biol. Chem. 283*, 19511–19520.

(27) Callaway, K. A., Rainey, M. A., Riggs, A. F., Abramczyk, O., and Dalby, K. N. (2006) Properties and regulation of a transiently assembled ERK2.Ets-1 signaling complex. *Biochemistry 45*, 13719–13733.

(28) Callaway, K., Abramczyk, O., Martin, L., and Dalby, K. N. (2007) The anti-apoptotic protein PEA-15 is a tight binding inhibitor of ERK1 and ERK2, which blocks docking interactions at the D-recruitment site. *Biochemistry 46*, 9187–9198.

(29) Abramczyk, O., Rainey, M. A., Barnes, R., Martin, L., and Dalby, K. N. (2007) Expanding the repertoire of an ERK2 recruitment site: cysteine footprinting identifies the D-recruitment site as a mediator of Ets-1 binding. *Biochemistry 46*, 9174–9186.

(30) Masterson, L. R., Cheng, C., Yu, T., Tonelli, M., Kornev, A., Taylor, S. S., and Veglia, G. (2010) Dynamics connect substrate recognition to catalysis in protein kinase A. *Nat. Chem. Biol. 6*, 821–828.

(31) Masterson, L. R., Mascioni, A., Traaseth, N. J., Taylor, S. S., and Veglia, G. (2008) Allosteric cooperativity in protein kinase A. *Proc. Natl. Acad. Sci. U.S.A. 105*, 506–511.

(32) Vajpai, N., Strauss, A., Fendrich, G., Cowan-Jacob, S. W., Manley, P. W., Grzesiek, S., and Jahnke, W. (2008) Solution conformations and

dynamics of ABL kinase-inhibitor complexes determined by NMR substantiate the different binding modes of imatinib/nilotinib and dasatinib. *J. Biol. Chem. 283*, 18292–18302.

(33) Vogtherr, M., Saxena, K., Hoelder, S., Grimme, S., Betz, M., Schieborr, U., Pescatore, B., Robin, M., Delarbre, L., Langer, T., Wendt, K. U., and Schwalbe, H. (2006) NMR characterization of kinase p38 dynamics in free and ligand-bound forms. *Angew. Chem., Int. Ed. 45*, 993–997.

(34) Akella, R., Min, X., Wu, Q., Gardner, K. H., and Goldsmith, E. J. (2010) The Third Conformation of p38alpha MAP Kinase Observed in Phosphorylated p38alpha and in Solution. *Structure 18*, 1571–1578.

(35) Wiesner, S., Wybenga-Groot, L. E., Warner, N., Lin, H., Pawson, T., Forman-Kay, J. D., and Sicheri, F. (2006) A change in conformational dynamics underlies the activation of Eph receptor tyrosine kinases. *EMBO J. 25*, 4686–4696.

(36) Takeuchi, K., Ng, E., Malia, T. J., and Wagner, G. (2007) 1-^{13}C amino acid selective labeling in a ^{2}H^{15}N background for NMR studies of large proteins. *J. Biomol. NMR 38*, 89–98.

(37) Salzmann, M., Pervushin, K., Wider, G., Senn, H., and Wuthrich, K. (1998) TROSY in triple-resonance experiments: new perspectives for sequential NMR assignment of large proteins. *Proc. Natl. Acad. Sci. U.S.A. 95*, 13585–13590.

(38) Clore, G. M., and Iwahara, J. (2009) Theory, practice, and applications of paramagnetic relaxation enhancement for the characterization of transient low-population states of biological macromolecules and their complexes. *Chem. Rev. 109*, 4108–4139.

(39) Shen, Y., and Bax, A. (2007) Protein backbone chemical shifts predicted from searching a database for torsion angle and sequence homology. *J. Biomol. NMR 38*, 289–302.

(40) Venters, R. A., Farmer, B. T., 2nd, Fierke, C. A., and Spicer, L. D. (1996) Characterizing the use of perdeuteration in NMR studies of large proteins: ^{13}C, ^{15}N and ^{1}H assignments of human carbonic anhydrase II. *J. Mol. Biol. 264*, 1101–1116.

(41) Piserchio, A., Dalby, K. N., and Ghose, R. (2011) Assignment of backbone resonances in a eukaryotic protein kinase – ERK2 as an illustrative example. *Methods Mol. Biol.*in press.

(42) Waas, W. F., and Dalby, K. N. (2001) Purification of a model substrate for transcription factor phosphorylation by ERK2. *Protein Expr. Purif. 23*, 191–197.

(43) Delaglio, F., Grzesiek, S., Vuister, G. W., Zhu, G., Pfeifer, J., and Bax, A. (1995) NMRPipe: a multidimensional spectral processing system based on UNIX pipes. *J. Biomol. NMR 6*, 277–293.

(44) Posas, F., Takekawa, M., and Saito, H. (1998) Signal transduction by MAP kinase cascades in budding yeast. *Curr. Opin. Microbiol. 1*, 175–182.

(45) Bardwell, A. J., Flatauer, L. J., Matsukuma, K., Thorner, J., and Bardwell, L. (2001) A conserved docking site in MEKs mediates high-affinity binding to MAP kinases and cooperates with a scaffold protein to enhance signal transmission. *J. Biol. Chem. 276*, 10374–10386.

(46) Balasu, M. C., Spiridon, L. N., Miron, S., Craescu, C. T., Scheidig, A. J., Petrescu, A. J., and Szedlacsek, S. E. (2009) Interface analysis of the complex between ERK2 and PTP-SL. *PLoS One 4*, e5432.

(47) Emrick, M. A., Lee, T., Starkey, P. J., Mumby, M. C., Resing, K. A., and Ahn, N. G. (2006) The gatekeeper residue controls autoactivation of ERK2 via a pathway of intramolecular connectivity. *Proc. Natl. Acad. Sci. U.S.A. 103*, 18101–18106.

(48) Yang, S. H., Yates, P. R., Whitmarsh, A. J., Davis, R. J., and Sharrocks, A. D. (1998) The Elk-1 ETS-domain transcription factor contains a mitogen-activated protein kinase targeting motif. *Mol. Cell Biol. 18*, 710–720.

(49) Yang, S. H., Whitmarsh, A. J., Davis, R. J., and Sharrocks, A. D. (1998) Differential targeting of MAP kinases to the ETS-domain transcription factor Elk-1. *EMBO J. 17*, 1740–1749.

(50) Zhang, J., Zhou, B., Zheng, C. F., and Zhang, Z. Y. (2003) A bipartite mechanism for ERK2 recognition by its cognate regulators and substrates. *J. Biol. Chem. 278*, 29901–29912.

(51) Slupsky, C. M., Gentile, L. N., Donaldson, L. W., Mackereth, C. D., Seidel, J. J., Graves, B. J., and McIntosh, L. P. (1998) Structure of the Ets-1 pointed domain and mitogen-activated protein kinase phosphorylation site. *Proc. Natl. Acad. Sci. U.S.A. 95*, 12129–12134.

(52) Lee, S., Warthaka, M., Yan, C., Kaoud, T., Piserchio, A., Ghose, R., Ren, P., and Dalby, K. N. (2011) A model of a MAPK•substrate complex in an active conformation: a computational and experimental approach. *PLoS One*in press.

(53) Seidel, J. J., and Graves, B. J. (2002) An ERK2 docking site in the Pointed domain distinguishes a subset of ETS transcription factors. *Genes Dev. 16*, 127–137.

(54) Formstecher, E., Ramos, J. W., Fauquet, M., Calderwood, D. A., Hsieh, J. C., Canton, B., Nguyen, X. T., Barnier, J. V., Camonis, J., Ginsberg, M. H., and Chneiweiss, H. (2001) PEA-15 mediates cytoplasmic sequestration of ERK MAP kinase. *Dev. Cell 1*, 239–250.

(55) Hill, J. M., Vaidyanathan, H., Ramos, J. W., Ginsberg, M. H., and Werner, M. H. (2002) Recognition of ERK MAP kinase by PEA-15 reveals a common docking site within the death domain and death effector domain. *EMBO J. 21*, 6494–6504.

(56) Bhattacharyya, R. P., Remenyi, A., Good, M. C., Bashor, C. J., Falick, A. M., and Lim, W. A. (2006) The Ste5 scaffold allosterically modulates signaling output of the yeast mating pathway. *Science 311*, 822–826.

(57) Heo, Y. S., Kim, S. K., Seo, C. I., Kim, Y. K., Sung, B. J., Lee, H. S., Lee, J. I., Park, S. Y., Kim, J. H., Hwang, K. Y., Hyun, Y. L., Jeon, Y. H., Ro, S., Cho, J. M., Lee, T. G., and Yang, C. H. (2004) Structural basis for the selective inhibition of JNK1 by the scaffolding protein JIP1 and SP600125. *EMBO J. 23*, 2185–2195.

(58) Hoofnagle, A. N., Resing, K. A., Goldsmith, E. J., and Ahn, N. G. (2001) Changes in protein conformational mobility upon activation of extracellular regulated protein kinase-2 as detected by hydrogen exchange. *Proc. Natl. Acad. Sci. U.S.A. 98*, 956–961.

(59) Davis, R. J. (2000) Signal transduction by the JNK group of MAP kinases. *Cell 103*, 239–252.